Journal of Himalayan Earth Sciences Volume 57, No. 1, 2024 pp. 60-78

Newly identified Active Faults in the Peshawar Basin

Muhammed Irfan Faiz[1], Sajjad Ahmed[1], Shuhab D. Khan[2], Fayaz Ali[1], Gohar Rehman[1], Adnan Khalid[1] and Taqueemul Haq Ali[3]

[1]*Department of Geology, University of Peshawar, KPK, Pakistan*

[2]*Department of Earth and Atmospheric Sciences, University of Houston, Houston, TX 77204, USA*

[3]*Department of Geology, Bacha Khan University, Charsada, KPK, Pakistan*

**Corresponding author: muhammedirfan@uop.edu.pk*

Submitted date: 10/10/2023 Accepted date: 11/03/2024 Published online: 31/03/2024

Abstract

Recent studies reveal that the Peshawar Basin, in the northwestern region of the Himalayas, is actively deforming in response to the ongoing tectonics of the Himalayas. Geological research on the Peshawar Basin has been limited despite thousands of reported low to moderate-magnitude earthquakes over the past two decades. After analyzing the Digital Elevation Model (DEM), seismic data, and geophysical data along with field observations, we have been able to identify six active faults that extend from the Southeast to the Northwest. Between 1978 and 2018, several earthquakes with a magnitude greater than 5 indicate neotectonics activity in the Peshawar Basin. Previous research has identified active faults only in the southern region of the Basin. This study presents a comprehensive mapping of active faults in the Peshawar Basin. These identified faults cut through the towns with the highest population density, given that the Peshawar Basin has only 10% of the exposed rocks. Field observations and fracture data from various infrastructures confirm that the Ghorghasti and Pir Sabak faults are thrust faults, while the Charsadda-Takhbhai, Mardan, Pir Piai, and Swabi faults are normal faults. Moreover, the alluvial deposits show normal faults and anticlinal folds, indicating widespread active deformation along these fault lines.

Keywords: Peshawar Basin, Active Faults, Digital Evaluation Mode (DEM), Alluvial deposits, and Active deformation.

1. Introduction

The boundaries of the Peshawar Basin in North Pakistan are bounded by longitude from 71°20'11.83" to 72°43'4.12" E and latitude from 33°45'31.33" to 34°32'14.22" N (Fig. 1). Numerous north-dipping faults in this area were created by deformation related to the Himalayan orogeny, and as a result, large-scale basins have developed in the Himalayan foothills. On the eastern side of the Hazara-Kashmir Syntaxis, the Peshawar basin has developed (Kohn, 2014; Searle and Schubert, 2015; Goscombe et al., 2018; Searle and Treloar, 2019). The Peshawar intermountain basin is oval-shaped, spans about 8200 km2, and is around 2.8 million years old. It resulted from the structural evolution of the Attock-Cherat Range (Cornwell, 1998) (Fig. 2).

From the fold-thrust belt to the northern landscape, the exposed rocks represent a transitional basin. Alluvial fans, flood plains, and young loess are layered over the lacustrine, deltaic, and fluvial deposits that make up the majority of the sediment in the basin. Similar to older rocks, these more recent deposits are also marked by folds and faults. A nearly complete sequence of rocks that extend from the Precambrian to the Triassic eras has been found in the Peshawar basin (Hussain et al., 1998). A thrust and folded range overlie the Peshawar intermontane basin in Pakistan on the southern margin of the Himalayas (Fig. 2).

This study aims to comprehend active tectonics, supported by recent seismic activity in the Peshawar Basin (WAPDA, 2018). A thorough understanding of active tectonics and the mitigation of related geologic hazards, such as earthquakes, requires an understanding of tectonic processes spanning several million years (Davis et al., 1993). Our main focus is on the active tectonic processes that hold the potential to initiate catastrophic events, even though these processes may also cause gradual disruption of the Earth's crust, leading to damage to human infrastructure through warping or tilting (Norris et al., 1990). The most hazardous kind of active tectonic activity that might cause a major earthquake is a massive earthquake. But even moderately sized earthquakes can cause disasters, especially when they occur in densely populated areas and if brittle materials (houses built of loose of sediment, particularly with high water content) or unreinforced cement blocks, bricks, or stones used for buildings are particularly hazardous. Earthquakes may occur in the coming decades due to faults, which may span several thousand to tens of thousands of years depending on the last occurrence. Active fault trace is a visible indication of ongoing deformation, usually caused by seismic activity. Significant insights into the movement and behavior of plate boundaries can be obtained by examining large databases of active fault data (Hussain and Yeats, 2002; Stirling et al., 2013). Hussain and Yeats (2002) identified active normal faults in the southern Peshawar Basin boundary. Among the faults are Garhi-Chandan, Uch-Khattak, Walai, and Misri-Banda. En-echelon pressure ridges are associated with these faults.

For the first time, we used hill shade images to identify active faults in the Peshawar basin. derived from DEM Pakistan. Based on an analysis of the Digital Evaluation Model (DEM) (Figure 3), field observations, earthquake data, and available geophysical data, six (06) faults were marked, namely Charsadda-Takh Bhai, Mardan, Pir Piai, Pir Sabak Swabi and Ghorghasti fault. The findings confirmed the existence of ongoing tectonic activity that could potentially trigger catastrophic events.

2. Methodology

The methods below were employed to find and identify active faults in the Peshawar Basin.

2.1 High-resolution Digital Evaluation Model (DEM) (12 m)

The Tandem-X DEM from the German Aerospace Agency was utilized in this study. To identify faults, the DEM was employed for generating hillshade images.

2.2 Earthquakes data

The seismic center of the Tarbella Dam Project provides earthquake data used to confirm active faults in the Peshawar Basin.

Data on earthquake location, date, time, depth, and magnitude were collected to understand Peshawar Basin's neo-tectonic activity.

2.3 Field observations

To validate the location of faults and trace any potential damages, field activities were carried out.

2.4 Geophysical data

2D move software was used to interpret the geophysical data that was obtained from OGDCL (Oil and Gas Development Company Limited).

3. Result and Interpretations

3.1 Fault Mapping from DEM and Hillshade

Using hillshade images obtained from a digital elevation model (DEM), six (06) active faults in the Peshawar Basin have been marked (Figs. 1 and 3). The method mimics topography light from several directions, improving lineaments in contrast to air photo interpretation. Shaded relief images are also essential for displaying landforms and identifying lineaments since they provide unimpeded bare-ground surfaces. Shaded-relief photos illuminated from a different light direction than the traditional sun location may assist in finding lineaments or Fault that are difficult to spot using traditional air photo interpretation methods. Field surveys were especially important with DEM and Hill-shade since possible faults highlighted in the Peshawar Basin passed through densely populated areas.

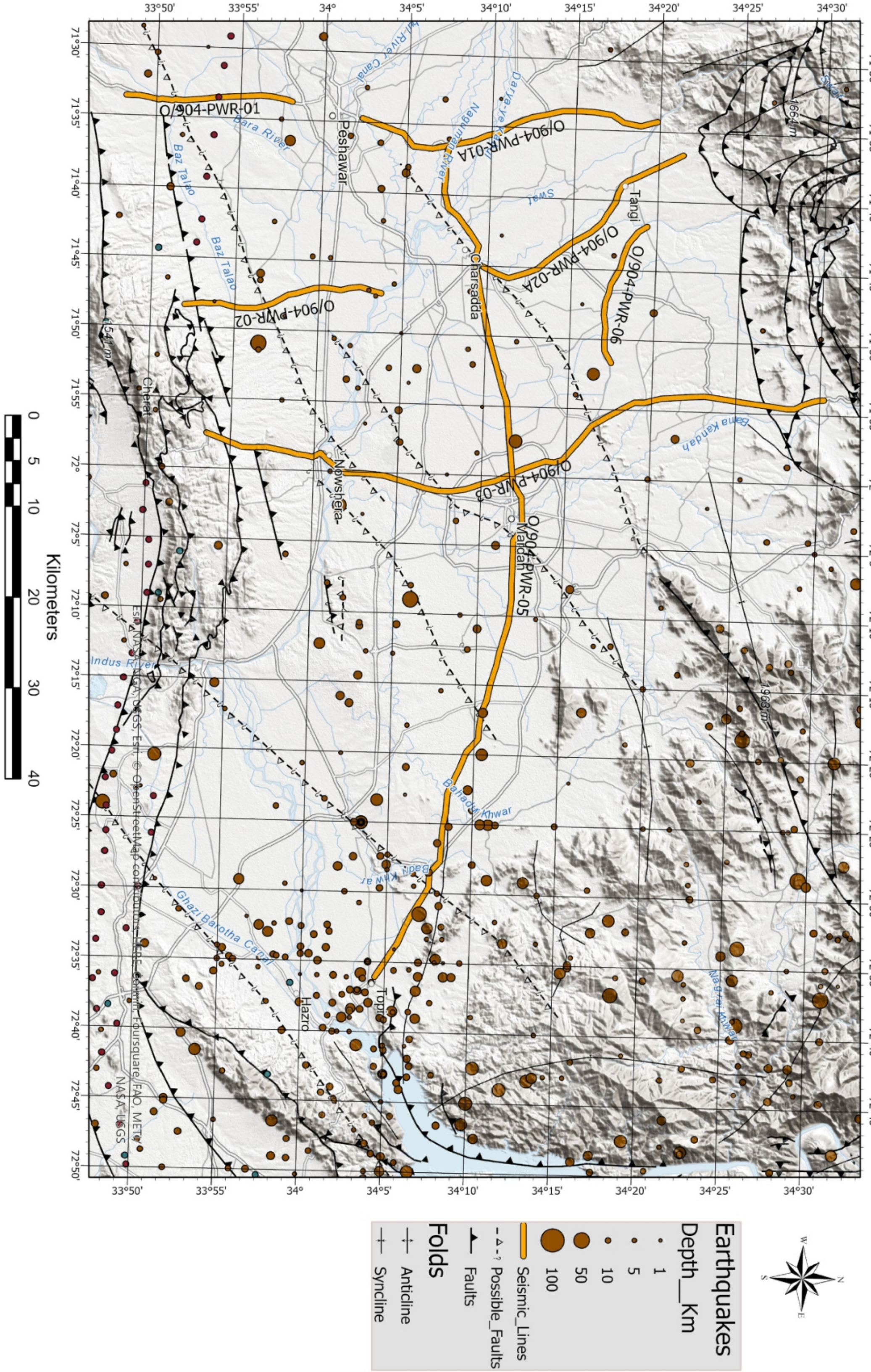

Fig. 1. Hill Shed image derived from DEM, showing possible faults. Earthquake data as well as the Seismic lines are plotted.

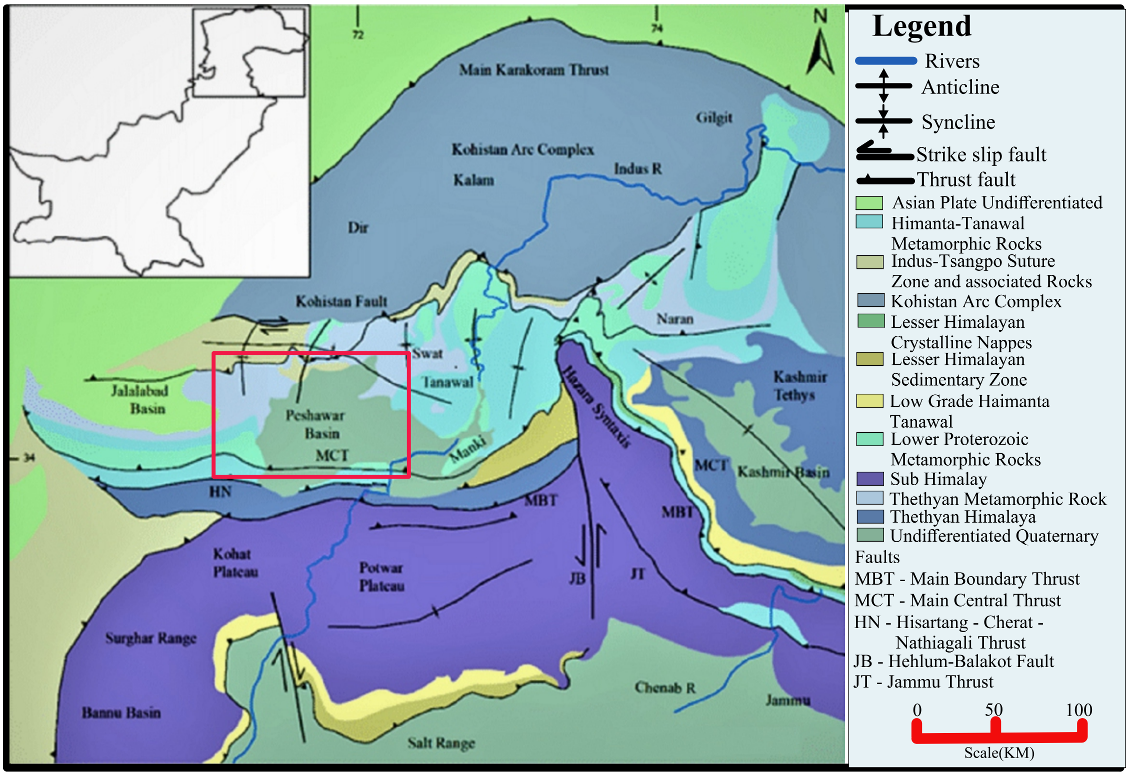

Fig. 2. Tectonic Map of North Pakistan (modified from Deipetro and Pogues, 2004); the study area is marked in the inset.

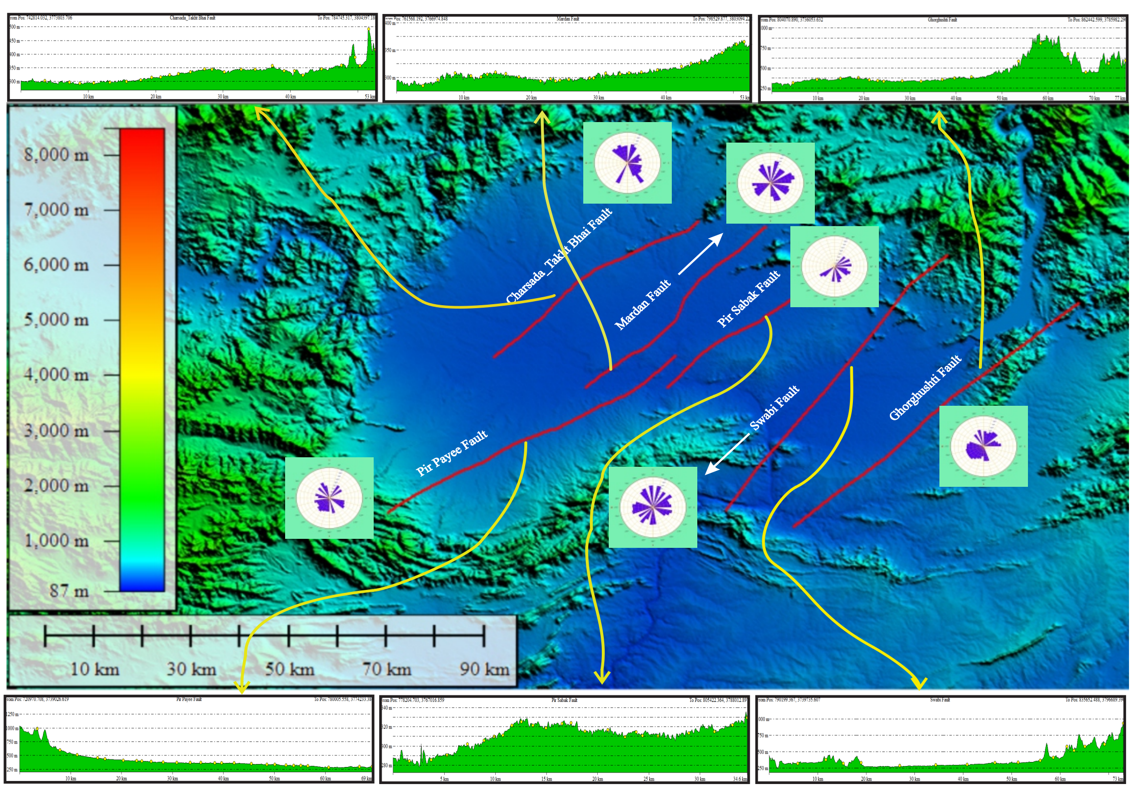

Fig. 3. Fracture data along active faults are displayed with Rose Diagrams, while the elevation profile of active faults is shown with yellow arrow lines on a DEM file.

3.2 Faults mapping from earthquake data

When the stress on a rock exceeds its strength, it ruptures, causing an earthquake and releasing energy as a result, faults are considered seismic sources (Stirling et al., 2013). According to Slemmons and Depolo (1986), surface faulting and strong ground motion correspond to active faulting, a geological hazard that has been connected to earthquakes. Active faults in the Peshawar Basin were confirmed using seismic data acquired from the Tarbella Dam Project (WAPDA, 2018). The data was collected from August 16, 1973, until December 27, 2018. During this time frame, more than 1200 earthquakes with magnitudes ranging from 3 to 5.7 on the Richter scale were recorded in the Peshawar Basin (Fig. 1). Earthquakes have occurred at varying magnitudes and locations in the 7.5 km radius along marked fault lines in the Peshawar Basin, with intervals ranging from one to several years. This illustration shows how faulting is similar to moving two rough boards past each other. The rough edges of the boards break off and cause slippage along the border, even if friction along the boundary between them may momentarily limit their motion.

3.3 Field Observations

In the Peshawar Basin, possible active faults mainly pass through crowded urban areas. Thus, fieldwork was done to observe the faults and their related characteristics, such as the many fracture sets that are present along each fault. Six different locations were observed on both sides of the fault to acquire fracture data. To determine the direction of stress, measurements and analyses were carried out on these fracture sets. An active fault could encounter both co-seismic rupture and inter-seismic deformation throughout an earthquake event. Tectonic strain in the crust may be received throughout the inter-seismic stage, which usually lasts for many hundreds to thousands of years. During the inter-seismic phase, strain is released, especially near active faults. Observing the transient deformation of the strain accumulation process is crucial for understanding active tectonic processes and associated energy release, especially given the increasing extent of human activities. The magnitude of the seismic hazard may also be influenced by the kind of local deformation present in a fault and the surrounding region. Recent alluvial deposits in the field showed many deformation indicators. The observation of normal faults and anticlinal folds confirms the active deformation on a larger scale, despite their small size (Fig. 4).

3.4 Active Faults in Peshawar Basin

Initially, the southern Peshawar Basin was found to have active faults by (Hussain and Yeats, 2002). Four left-stepping ridges that run diagonally along the imbricate thrust structures of the Attock-Cherat Range preceded these faults.

The Peshawar basin's recent un-lithified sediments are folded and faulted, displaying lacustrine, fluvial, and alluvial fan deposits, as well as more recent alluvial-fan gravels. Advanced techniques were used to identify six new active faults in the Peshawar Basin, covering it completely from southwest to northeast (Figs. 3 and 5). The active faults Charsadda-Takht Bhai, Mardan, and Pir Piai have been confirmed by the seismic lines O/904-PWR-01, O/904-PWR-02, and O/904-PWR-05.

3.4.1 Charsadda-Takht Bhai fault

The fault has originated in the Daman-e-Hindi region, close to Peshawar, and extends through the urban areas of Takht Bhai and Charsadda, this is the reason for the name. The fault was initially detected by using a hillshade images acquired from DEM images. Seismic data from the Tarbela Seismic Centre supported the fact that between 1974 and 2009, there were 19 earthquakes of magnitudes ranging from 3.0 to 4.5 within a 7.5 km radius around this fault Only a few of the earthquakes happened at depths of more than 20 km, while most of them were at shallow depths of less than 10 km.

This conclusively confirms that tectonics is active (WAPDA, 2018) (Fig. 5 and Table 1). Fracture data was collected from infrastructure in six locations on both sides of the Charsadda - Takht Bhai Fault during field observations. The data indicates that fractures dip either in the northwestern or southeastern quadrant. The Charsadda-Takht Bhai fault is perpendicular to some systematic fracture orientations that dip either northward or southward. The majority of the fractures that occur along this fault are Mode-1 fractures. The fault is an extensional Normal fault with fractures ranging from 2 cm to 5 cm in dilation separation. The seismic line O/904-PWR-05 provides evidence of an active fault.

3.4.2 Mardan fault

The Mardan district's densely populated urban areas are traversed by the Mardan active faults. This was identified using hillshed images derived from DEM. From 1973 to 2009, 24 earthquakes ranging from 3 to 4.4 magnitude on the Richter scale triggered areas within a 7.5 km radius of this fault (WAPDA, 2018). Additionally, evidence of active tectonics is shown in earthquakes that occur at depths shallower than 10 km (Table 2 and Fig. 5). Assessing seismic dangers and risks in urban areas requires close observation of active faults. The intent of the fieldwork was to study the infrastructure surrounding the fault areas.

Numerous structural problems, such as tilting and fractures, were identified in the infrastructure and recent deposits. Fracture data was collected from six different stations. This fault has been confirmed by interpreting the available geophysical data in the area using 2D Move software (Fig. 5). The majority of fractures parallel to the fault indicate an active Normal fault in the quadrant to the east (Fig. 5).

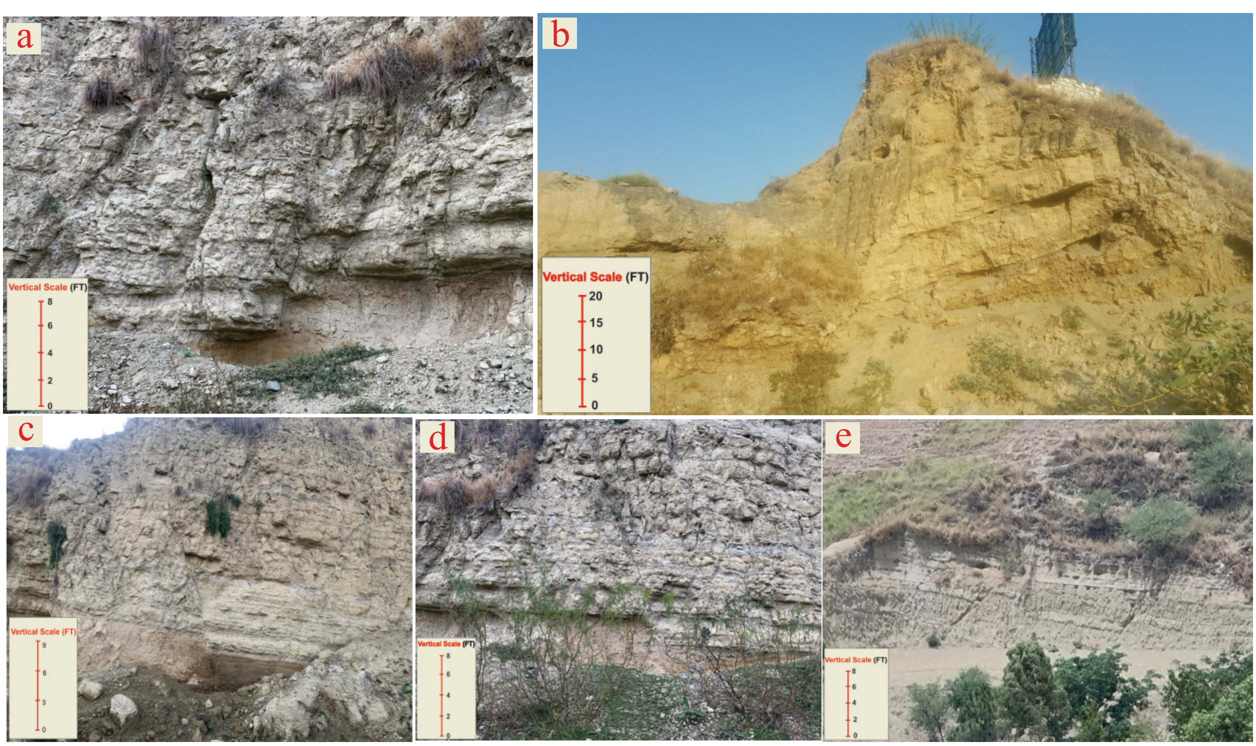

Fig. 4. Field phograph showing: (a) Horst and Graben Structure in the recent deposit along the marked Pir piai active fault, (b) tilting in recent deposits near Nowshera Reef area, district Nowshera, (c) Normal fault in the alluvium deposits along a long the Misri Banda, (d) Normal fault in recent deposits along Ghorghasti fault, and (e) Normal faults in recent deposits along the Pir Piai fault.

Table. 1. Earthquake data along Charsadda-Takht Bhai fault.

Sr. No.	Date	Time (PST)	Latitude	Longitude	Depth (km)	Magnitude
1	2/11/1984	13:35	34.262	71.792	0.00	4.50
2	7/14/1978	11:46	34.125	71.600	5.00	4.00
3	6/13/1974	18:01	34.083	71.642	20.00	3.80
4	3/23/2009	23:57	34.198	71.839	5.00	3.80
5	2/16/1976	22:20	34.275	71.875	35.00	3.70
6	9/18/2008	9:47	34.332	71.999	9.83	3.70
7	3/23/1986	17:22	34.027	71.600	10.00	3.50
8	12/8/1974	14:10	34.200	71.958	40.00	3.40
9	11/22/1975	23:30	34.150	71.850	5.00	3.30
10	4/16/1977	8:44	34.358	71.950	20.00	3.20
11	7/4/1987	15:57	34.258	71.900	5.00	3.20
12	3/6/2006	10:15	34.151	71.781	9.61	3.20
13	4/19/2008	23:27	34.059	71.662	14.34	3.20
14	11/9/1974	17:27	34.180	71.713	0.00	3.10
15	5/9/1981	13:28	34.062	71.700	5.00	3.00
16	2/18/1984	3:29	34.085	71.635	10.00	3.00
17	1/24/1989	6:30	34.057	71.607	10.00	3.00
18	11/18/1999	6:16	34.392	72.032	0.05	3.00
19	9/26/2000	0:00	34.349	72.152	5.00	3.00

Table. 2. Earthquake data along Mardan fault.

Sr. No.	Date	Time (PST)	Latitude	Longitude	Depth (km)	Magnitude
1	5/19/1975	19:03	34.075	71.9330	0.00	4.4
2	12/31/1983	2:55	34.017	71.8420	5.00	4.3
3	1/4/1984	18:53	34.333	72.2500	10.00	4.2
4	12/14/1975	21:32	34.258	72.1330	20.00	3.9
5	12/12/2000	21:38	34.057	71.7900	4.06	3.8
6	7/14/1984	16:02	34.143	72.0550	10.00	3.7
7	5/27/1997	1:16	34.225	72.1700	4.89	3.5
8	10/30/1974	11:14	34.133	72.0000	0.00	3.4
9	3/21/1986	2:31	34.283	72.2000	5.00	3.4
10	3/29/1979	16:18	34.083	71.9250	15.00	3.3
11	11/11/1982	12:47	34.033	71.8500	5.00	3.3
12	6/25/2005	17:19	34.085	71.9630	12.98	3.3
13	8/12/2000	11:00	34.162	71.9730	5.00	3.2
14	1/5/2009	8:57	34.030	71.8900	14.00	3.2
15	9/5/2009	0:53	34.300	72.2000	10.00	3.2
16	3/20/1974	7:05	33.967	71.8170	0.00	3.1
17	5/20/1975	6:24	34.100	71.8750	20.00	3.1
18	5/22/1975	5:00	34.050	71.9420	0.00	3.1
19	5/22/1975	2:44	34.092	71.8920	0.00	3.1
20	1/8/1981	11:13	34.042	71.9000	5.00	3.1
21	5/6/1985	8:36	34.072	71.8750	10.00	3.1
22	1/12/1989	10:25	34.367	72.2320	10.00	3.1
23	11/23/1973	10:05	34.083	71.8330	0.00	3.0
24	10/13/1982	19:36	34.183	72.0830	20.00	3.0

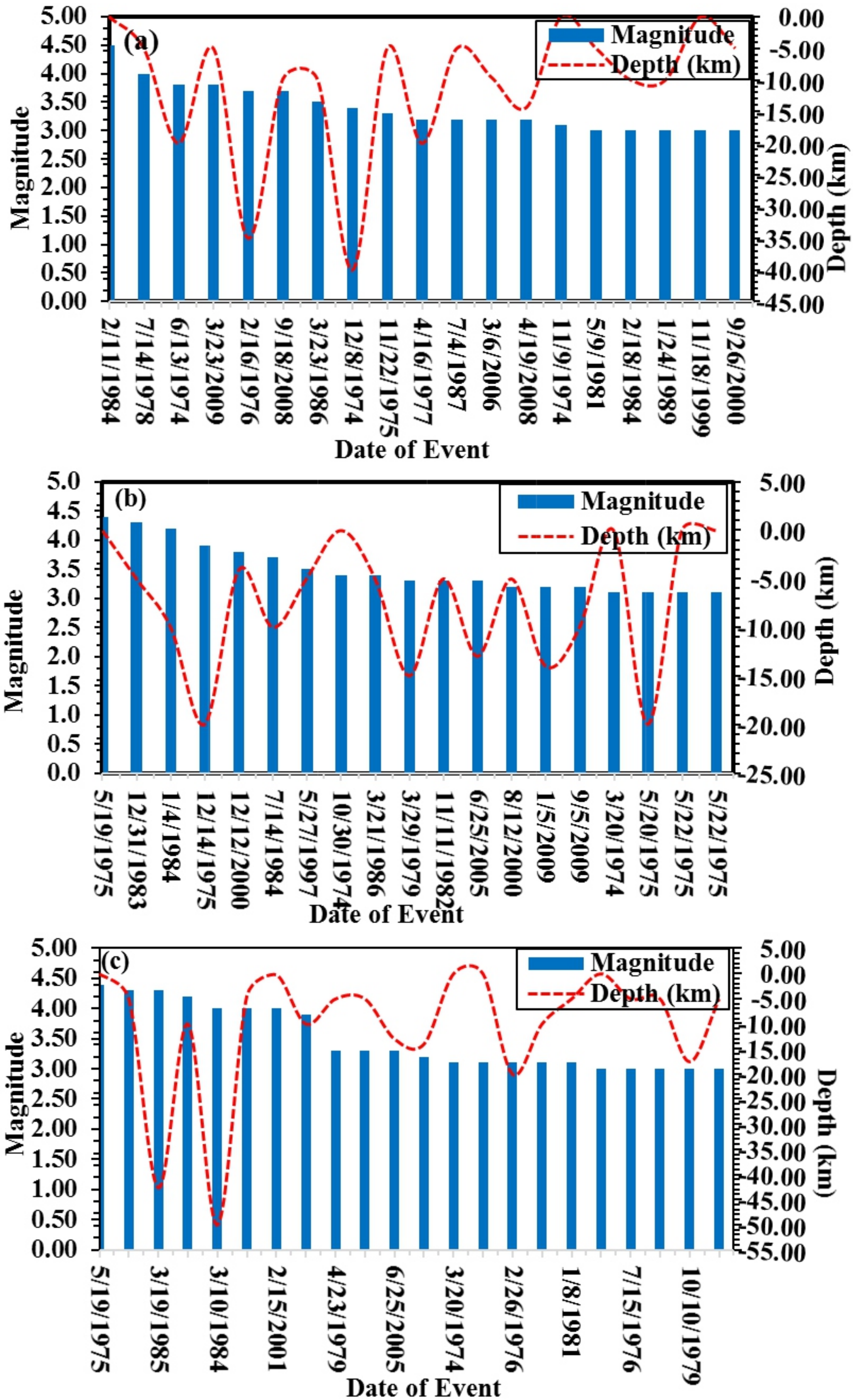
(a)
Magnitude
Depth (km)
Date of Event
2/11/1984
7/14/1978
6/13/1974
3/23/2009
2/16/1976
9/18/2008
3/23/1986
12/8/1974
11/22/1975
4/16/1977
7/4/1987
3/6/2006
4/19/2008
11/9/1974
5/9/1981
2/18/1984
1/24/1989
11/18/1999
9/26/2000
(b)
Magnitude
Depth (km)
Date of Event
5/19/1975
12/31/1983
1/4/1984
12/14/1975
12/12/2000
7/14/1984
5/27/1997
10/30/1974
3/21/1986
3/29/1979
11/11/1982
6/25/2005
8/12/2000
1/5/2009
9/5/2009
3/20/1974
5/20/1975
5/22/1975
5/22/1975
(c)
Magnitude
Depth (km)
Date of Event
5/19/1975
3/19/1985
3/10/1984
2/15/2001
4/23/1979
6/25/2005
3/20/1974
2/26/1976
1/8/1981
7/15/1976
10/10/1979

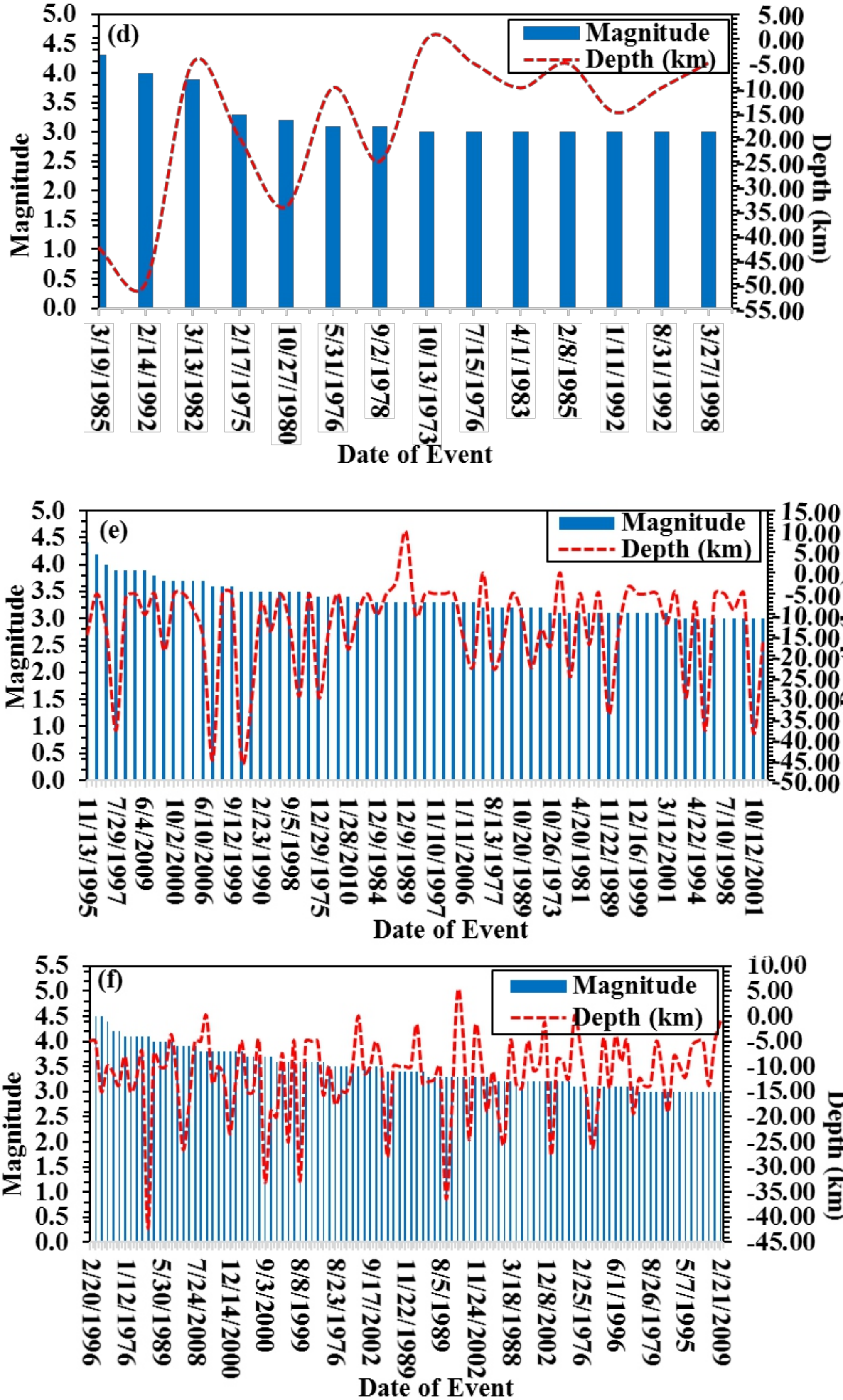

Fig. 5. Variation of magnitude and depth of event at: a) Charsadda-Takht Bhai fault, b) Mardan fault, c) Pir Piai fault, d) Pir Sabak fault, e) Swabi fault, and f) Ghorghushti fault.

3.4.3 Pir Piai fault

As the third documented active fault in the Peshawar Basin, its name derived as it passes mostly through Pir Piai areas. To validate and support this fault, the same method and standards were used. This fault triggered 22 earthquakes from 1973 to 2009, ranging in magnitude from 3.0 to 4.4 on the Richter scale within a 7.5 km radius of a 45 km long fault (Table 3 and Fig. 5). The earthquakes occurred at an average depth of 10 km, with most happening below 10 km and very few going beyond 40 km. This indicates that there is shallow-depth seismic activity associated with active faults. The team conducted fieldwork along the fault line and collected fracture data at six points on either side of the infrastructure. Active faults have been observed along this fault during field observations on smaller scales, validating active.

Faulting on a larger scale (Fig. 6). After analyzing the fracture data, it was found that almost all of the fractures have a parallel dip to the Pir Piai Fault. Because of their wide distribution, these fractures do not indicate a particular direction and this fault is a Normal active fault. In this study, 2D move software was used to interpret seismic lines O/904-PWR-01, O/904-PWR-02, and O/904-PWR-05 confirm a fault. In this study, 2D move software was used to interpret seismic lines O/904-PWR-01, O/904-PWR-02, and O/904-PWR-05 confirm a fault (Fig. 6).

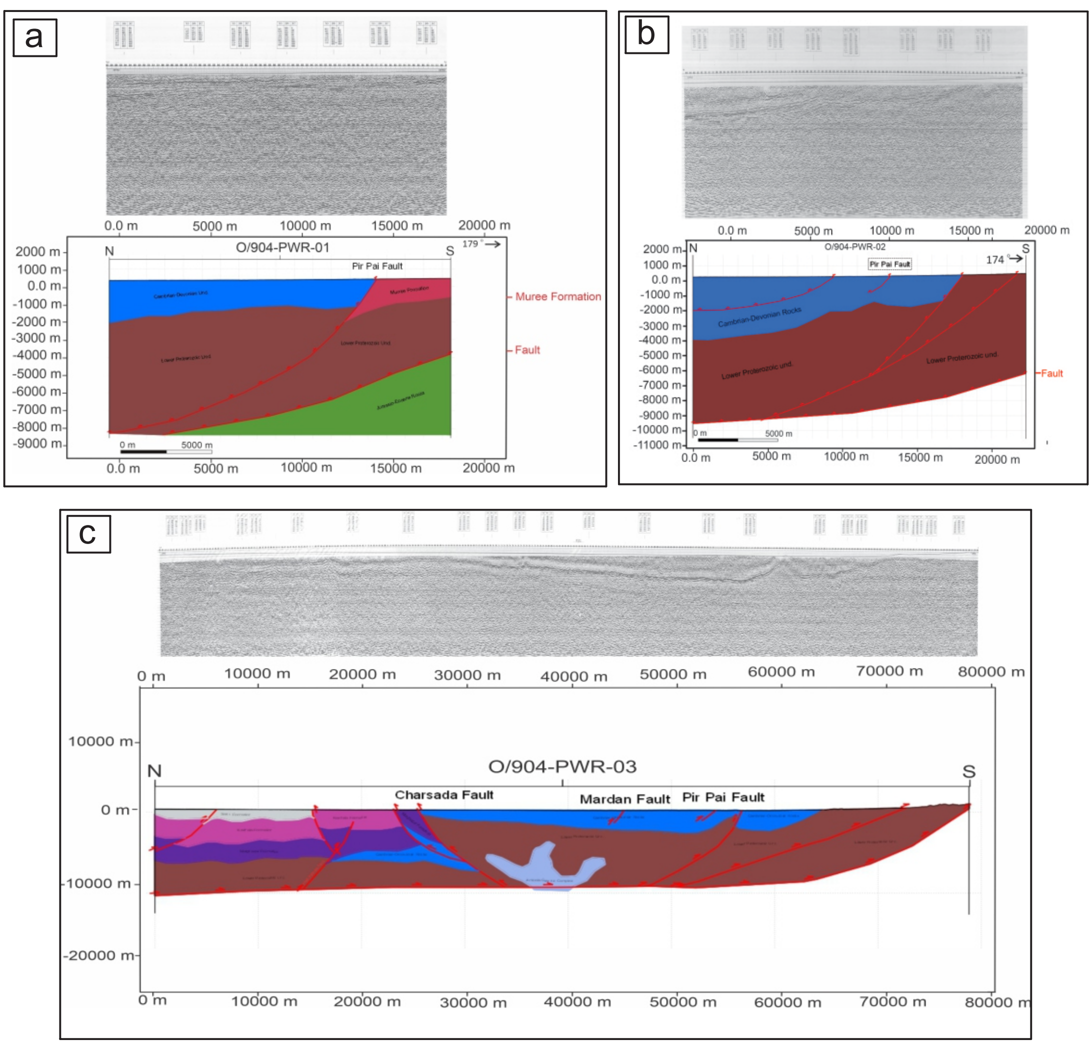

Fig. 6. Geo-seismic Interpreted Lines shows Charsadda, Pir Pai fault and Mardan fault: (a) O/904-PWR-01, (b) O/904-PWR-02, and (c) O/904-PWR-03.

Table. 3. Earthquake data along Pir Piai fault

Sr. No	Date	Time (PST)	Latitude	Longitude	Depth (km)	Magnitude
1	5/19/1975	19:03	34.075	71.933	0.00	4.40
2	12/31/1983	2:55	34.017	71.842	5.00	4.30
3	3/19/1985	9:37	34.027	72.040	42.60	4.30
4	9/20/1984	21:07	33.942	71.858	10.00	4.20
5	3/10/1984	4:25	33.942	71.850	50.00	4.00
6	1/27/1986	17:28	33.860	71.605	4.40	4.00
7	2/15/2001	7:50	33.897	71.802	0.19	4.00
8	12/25/1975	17:56	33.942	71.775	10.00	3.90
9	4/23/1979	9:40	33.967	71.917	5.00	3.30
10	11/11/1982	12:47	34.033	71.850	5.00	3.30
11	6/25/2005	17:19	34.085	71.963	12.98	3.30
12	1/5/2009	8:57	34.030	71.890	14.00	3.20
13	3/20/1974	7:50	33.967	71.817	0.00	3.10
14	5/22/1975	2:42	34.050	71.942	0.00	3.10
15	2/26/1976	21:29	33.942	71.767	20.00	3.10
16	2/26/1976	21:34	33.942	71.767	20.00	3.10
17	5/31/1976	1:12	34.025	72.050	10.00	3.10
18	1/8/1981	11:13	34.042	71.900	5.00	3.10
19	10/13/1973	15:34	34.050	72.050	0.00	3.00
20	7/15/1976	11:56	34.017	72.000	5.00	3.00
21	10/10/1979	1:06	33.850	71.667	17.50	3.00
22	5/27/2002	9:00	33.954	71.705	5.00	3.00

3.4.4 Pir Sabak fault

This fault extends for 34 km, starting from Pir Sabak area of Nowshera, passing through several urban areas. The same approach and techniques used for marking other faults have been used to mark this fault. Between 1973 and 1998, fourteen earthquakes were recorded along this fault within a 7.5 km radius, and this seismic activity validates the fault. The earthquakes that occurred had Richter magnitudes that ranged between 3.00 to 4.3. Few of them happened deeper than 20 km, while most happened at shallow depths of 10 km or less (Table 4 and Fig. 5). The existence of active tectonics in the form of an active fault is confirmed by shallow seismic activity. During a thorough field observation along the fault line, several cracks in the infrastructure were identified. Additionally, recent deposits showed evidence of tilting and small-scale normal faults, as depicted in Figure 4. Although these features were relatively small, they indicate that significant active deformation is occurring on a larger scale. Fracture data has been collected from six locations on both sides of the active fault that has been marked. The analysis reveals that there are only a few fractures in the western quadrant, while the majority of them dip towards the southeast. Based on this data, the fault is considered to be a Normal Active fault.

3.4.5 Swabi fault

With a length of 72 km and passing through the majority of Swabi's urban area, the Swabi fault is the longest of the six active faults. The same techniques and approaches were initially used to identify this fault. According to earthquake data, the existence of a fault was confirmed by 72 ground tremors that occurred within a 7.5 km radius from 1993 to 2010. The magnitudes of these earthquakes ranged from

3.0 to 4.4 on the Richter scale. Most of the earthquakes occurred at shallow depths of less than 10 km, with only a few happening at depths greater than 20 km. The fault is active as suggested by shallow seismic activity (Table 5 and Fig. 5). It was observed during the fieldwork that the left side of the fault line had subsided. Apart from collecting fracture data, a closer study of the area revealed that the newly constructed buildings had sunk, most likely due to this fault. Only three years old, the NADRA NRC Swabi office building has a 7 cm subsidence on its eastern side, suggesting an approximate 2-centimeter per year subsidence (Fig. 7).

Despite taking all necessary safety precautions during construction, a recently built home in the area also experienced subsidence. Even the use of iron and concrete on the ground floor was ineffective, indicating that the ground was sinking along that side of the fault. Field observations on Topi Road showed that the school building had vertical fractures, and the southern side of the school subsided similarly to the NADRA NRC Swabi office.

Six different stations on either side of the Swabi fault were used to acquire fracture data. An analysis of this data indicates that most fractures are dipping toward the trend of the fault. Although there is a lot of fracture data, it is concentrated in the western quadrant, which is also where various areas' subsidence is visible. This could be due to the typical characteristics of the Normal fault.

Table. 4. Earthquake data along Pir Sabak fault.

Sr. No.	Date	Time (PST)	Latitude	Longitude	Depth (km)	Magnitude
1	3/19/1985	9:37	34.027	72.040	42.60	4.3
2	2/14/1992	18:50	34.100	72.150	50.00	4.0
3	3/13/1982	0:29	34.133	72.258	5.00	3.9
4	2/17/1975	21:27	34.167	72.183	20.00	3.3
5	10/27/1980	13:21	34.175	72.333	34.30	3.2
6	5/31/1976	1:12	34.025	72.050	10.00	3.1
7	9/2/1978	8:55	34.175	72.283	25.00	3.1
8	10/13/1973	15:34	34.050	72.050	0.00	3.0
9	7/15/1976	11:56	34.017	72.000	5.00	3.0
10	4/1/1983	23:21	34.100	72.133	10.00	3.0
11	2/8/1985	21:04	34.150	72.167	5.00	3.0
12	1/11/1992	15:53	34.087	72.180	15.00	3.0
13	8/31/1992	18:35	34.158	72.208	10.00	3.0
14	3/27/1998	23:02	34.084	72.215	4.92	3.0

Table. 5. Earthquake data along Swabi fault.

Sr. No	Date	Time (PST)	Latitude	Longitude	Depth (km)	Magnitude
1	11/13/1995	21:35	34.050	72.417	15.00	4.4
2	11/29/2005	0:28	33.797	72.155	14.22	4.3
3	10/10/2010	2:44	33.997	72.348	5.00	4.2
4	11/11/2000	17:28	34.168	72.465	13.97	4.0
5	7/29/1997	23:46	34.057	72.417	37.88	3.9
6	5/26/1999	9:51	33.919	72.286	5.95	3.9
7	7/23/2000	2:20	34.057	72.417	5.00	3.9
8	6/4/2009	23:26	34.020	72.390	10.00	3.9
9	8/10/2000	3:32	34.057	72.417	5.00	3.8
10	5/22/2000	4:47	34.057	72.417	18.72	3.7
11	10/2/2000	8:07	34.084	72.473	5.00	3.7
12	10/3/2000	21:28	34.057	72.417	5.00	3.7
13	12/21/2000	21:10	34.084	72.455	8.79	3.7
14	6/10/2006	3:38	34.123	72.470	15.55	3.7
15	7/3/1974	18:55	34.308	72.617	45.00	3.6
16	3/25/1984	21:32	34.233	72.558	5.00	3.6
17	9/12/1999	7:09	34.057	72.513	5.00	3.6
18	2/11/1978	12:54	34.117	72.525	45.00	3.5
19	2/25/1985	0:27	34.258	72.592	31.30	3.5
20	2/23/1990	19:29	33.852	72.158	7.60	3.5
21	5/31/1992	16:13	33.725	72.098	13.90	3.5
22	5/27/1997	22:22	34.057	72.417	5.00	3.5
23	9/5/1998	2:38	34.057	72.417	12.67	3.5
24	6/20/1999	3:16	34.134	72.579	29.59	3.5
25	5/7/2001	22:21	34.140	72.555	5.00	3.5
26	12/29/1975	16:08	34.125	72.542	30.00	3.4
27	11/18/1990	10:18	34.077	72.457	14.00	3.4
28	3/20/2001	2:04	34.125	72.555	5.00	3.4
29	1/28/2010	8:54	34.265	72.585	18.30	3.4
30	11/17/1973	20:49	34.158	72.583	10.00	3.3
31	8/28/1981	7:44	33.817	72.208	5.00	3.3
32	12/9/1984	11:10	33.972	72.400	10.00	3.3
33	5/6/1985	8:24	33.817	72.117	5.00	3.3
34	2/1/1989	22:52	34.035	72.335	2.00	3.3
35	12/9/1989	20:11	34.057	72.417	10.00	3.3
36	11/28/1994	14:50	34.110	72.477	10.00	3.3
37	1/12/1996	10:00	34.057	72.417	5.00	3.3
38	11/10/1997	22:15	34.057	72.417	5.00	3.3
39	11/28/1999	0:38	34.057	72.417	5.00	3.3
40	3/9/2000	19:04	34.057	72.417	5.00	3.3
41	1/11/2006	20:51	34.133	72.440	16.20	3.3
42	11/15/2009	8:50	34.035	72.470	22.32	3.3
43	3/18/1975	15:00	34.100	72.383	0.00	3.2
44	8/13/1977	14:22	34.083	72.467	22.50	3.2
45	1/31/1978	17:46	34.125	72.475	17.50	3.2

46	3/8/1988	15:30	33.758	72.133	5.00	3.2
47	10/20/1989	23:21	34.270	72.698	10.00	3.2
48	9/6/1996	9:09	33.908	72.255	22.82	3.2
49	11/18/2009	3:32	34.077	72.495	13.63	3.2
50	10/26/1973	12:20	34.050	72.458	17.50	3.1
51	7/27/1975	1:28	34.142	72.583	0.00	3.1
52	2/5/1977	23:24	34.200	72.558	25.00	3.1
53	4/20/1981	17:22	34.192	72.533	5.00	3.1
54	2/21/1985	12:10	34.265	72.582	17.20	3.1
55	2/21/1985	1:27	34.268	72.573	5.00	3.1
56	11/22/1989	9:17	34.072	72.390	33.90	3.1
57	8/30/1997	16:38	34.057	72.417	14.75	3.1
58	7/26/1998	9:39	34.057	72.417	3.45	3.1
59	12/16/1999	10:47	34.057	72.417	5.00	3.1
60	3/9/2000	19:07	34.057	72.417	5.00	3.1
61	10/11/2000	0:00	34.111	72.492	5.00	3.1
62	3/12/2001	14:27	34.139	72.540	12.16	3.1
63	12/12/1980	21:19	34.233	72.667	5.00	3.0
64	9/21/1983	12:56	34.183	72.483	30.00	3.0
65	4/22/1994	12:19	33.775	72.165	7.05	3.0
66	3/7/1997	8:49	34.057	72.417	37.94	3.0
67	10/30/1997	7:49	34.057	72.417	5.00	3.0
68	7/10/1998	9:23	34.057	72.417	4.99	3.0
69	9/6/2000	0:32	34.134	72.500	8.92	3.0
70	2/17/2001	13:00	34.057	72.417	5.00	3.0
71	10/12/2001	3:32	34.057	72.417	38.59	3.0
72	6/28/2007	14:09	34.136	72.515	16.46	3.0

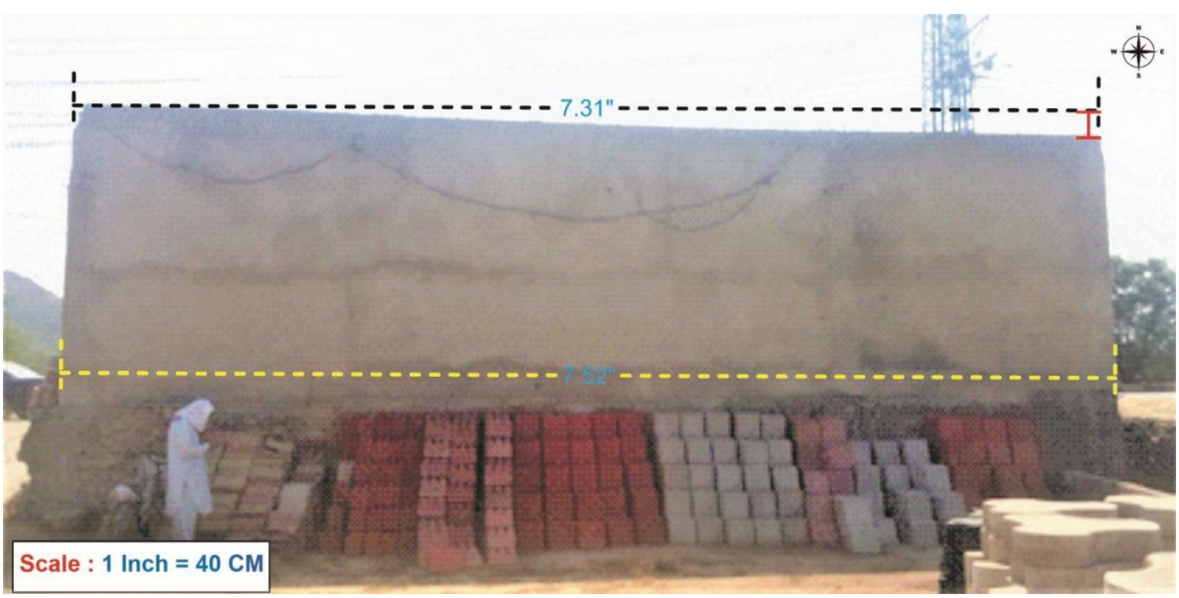

Fig. 7. A photograph was taken at a 90° angle showing a 7cm subsidence on the eastern side of the building.

3.4.6 Ghorghushti Fault

This fault extends for almost 45 km in the urban area of the southeastern Peshawar basin. The fault was identified using hillshade images derived from a digital elevation model (DEM), and confirmed by significant earthquakes that occurred within 7.5 km radius of the fault between 1973 and 2017 (WAPDA, 2018). The earthquakes in the area have a magnitude between 3.00 and 5.2 on the Richter scale (Table 6 and Fig. 5). Most of them occur at depths less than 10 km, with only a few deeper than 20 km, indicating active faulting. During our fieldwork, we noticed that electric poles were tilting, and the metaled road was subsiding along the fault line. Moreover, a newly constructed house boundary wall, which was not older than three years, had significant vertical cracks in an eastward direction (Fig. 7). The occurrence of these earthquakes suggests that the area is undergoing active deformation. We collected fracture data at six (06) points on both sides of the fault and analyzed it. The fractures' data analysis shows that:

1. The Ghorghushti fault runs parallel to the dips of the fractures.

2. Most of the southwestward dips are located on the opposite side of the orientations.

3. There are few or no openings in the fractures, which is indicative of compressive shear stress.

4. According to statistics, a thrust or reverse fault is the most probable cause.

Table. 6. Earthquake data along Ghorghashti fault.

Sr. No.	Date	Time (PST)	Latitude	Longitude	Depth (km)	Magnitude
1	2/20/1996	7:50	34.050	72.667	5.00	5.2
2	12/2/1974	17:58	34.100	72.942	50.00	4.5
3	3/3/1977	18:39	34.042	72.875	5.00	4.5
4	4/14/1982	13:31	33.983	72.667	15.00	4.5
5	11/15/1974	15:02	33.878	72.525	10.00	4.4
6	9/2/1982	14:43	33.933	72.583	11.20	4.2
7	4/10/1997	6:38	33.929	72.580	13.76	4.2
8	1/12/1976	12:58	33.917	72.567	8.00	4.1
9	8/21/1976	2:50	34.053	72.850	15.00	4.1
10	8/18/1979	16:04	34.033	72.667	12.50	4.1
11	10/10/1990	2:56	34.037	72.750	7.40	4.1
12	8/2/2014	7:08	33.800	72.400	42.00	4.1
13	12/8/1988	1:13	34.067	72.833	7.50	4.0
14	5/30/1989	3:23	34.100	72.867	10.00	4.0
15	6/26/1993	15:35	34.012	72.810	10.00	4.0
16	1/11/1999	21:00	34.057	72.865	3.71	4.0
17	11/8/1973	10:14	34.075	72.708	13.00	3.9
18	10/19/1989	14:54	34.132	72.852	26.49	3.9
19	4/1/1990	12:07	33.922	72.570	17.50	3.9
20	7/24/2008	0:23	34.132	72.852	5.00	3.9
21	12/2/1973	5:00	34.083	72.750	5.00	3.8
22	6/19/1974	23:35	33.833	72.383	0.00	3.8
23	1/10/1993	22:46	34.085	72.717	13.07	3.8
24	5/7/1995	15:55	34.028	72.648	10.00	3.8
25	5/7/1995	16:15	34.023	72.740	12.05	3.8

26	12/14/2000	17:22	34.132	72.880	23.33	3.8
27	1/23/2001	21:14	34.024	72.663	13.18	3.8
28	2/14/2007	13:14	33.958	72.592	5.00	3.8
29	1/23/1974	16:04	34.067	72.800	15.00	3.7
30	3/17/1976	2:56	34.033	72.633	15.00	3.7
31	8/23/2000	19:32	34.132	72.852	5.00	3.7
32	9/3/2000	1:24	34.127	72.870	32.76	3.7
33	10/30/2000	20:07	34.084	72.815	18.96	3.7
34	4/8/1974	0:53	33.845	72.567	20.00	3.6
35	4/11/1976	3:43	33.967	72.633	7.50	3.6
36	11/23/1977	15:27	34.083	72.833	25.00	3.6
37	6/30/1985	7:56	34.067	72.767	5.00	3.6
38	8/8/1999	18:12	34.057	72.683	32.70	3.6
39	8/19/1999	0:00	34.072	72.902	5.00	3.6
40	12/20/1999	7:19	33.734	72.232	5.00	3.6
41	3/3/2003	1:37	33.973	72.540	5.00	3.6
42	5/22/2012	7:55	34.064	72.875	8.67	3.6
43	3/21/2017	10:56	33.914	72.598	15.67	3.6
44	11/28/1973	4:02	33.917	72.583	10.00	3.5
45	8/23/1976	13:01	34.067	72.842	17.50	3.5
46	5/19/1986	12:28	34.032	72.733	15.00	3.5
47	12/30/1986	18:05	33.810	72.367	15.00	3.5
48	12/5/1989	7:46	34.085	72.717	10.00	3.5
49	5/24/1996	21:25	33.837	72.380	0.04	3.5
50	9/6/2000	18:14	34.097	72.822	11.26	3.5
51	9/17/2002	4:19	33.734	72.232	10.13	3.5
52	9/8/2008	11:17	33.734	72.232	5.00	3.5
53	9/18/2008	14:27	34.036	72.747	10.49	3.5
54	10/2/1974	19:07	33.967	72.550	28.00	3.4
55	9/2/1975	7:55	34.075	72.775	10.00	3.4
56	11/9/1989	1:48	34.083	72.717	10.00	3.4
57	11/22/1989	13:34	34.085	72.717	10.00	3.4
58	11/3/1990	9:56	34.132	72.852	10.00	3.4
59	7/26/1997	7:59	33.854	72.490	1.64	3.4
60	5/27/2012	14:29	34.074	72.812	13.33	3.4
61	6/19/1974	1:27	34.000	72.575	13.00	3.3
62	2/22/1975	22:21	34.017	72.625	12.50	3.3
63	8/5/1989	12:19	34.132	72.852	10.00	3.3
64	8/22/1989	0:26	34.110	72.833	36.20	3.3
65	6/11/1990	10:19	34.100	72.735	18.40	3.3
66	5/8/1996	17:33	34.132	72.850	5.00	3.3
67	2/4/2000	18:59	33.734	72.232	5.00	3.3
68	10/12/2000	17:01	34.084	72.717	24.51	3.3
69	11/24/2002	16:56	34.132	72.852	2.16	3.3
70	4/6/2007	2:53	33.745	72.310	8.66	3.3
71	7/2/2008	17:06	33.734	72.232	18.91	3.3
72	4/14/1975	4:57	34.025	72.767	11.00	3.2

73	9/15/1975	22:32	34.000	72.633	20.00	3.2
74	11/28/1978	8:39	34.042	72.650	25.00	3.2
75	3/18/1988	0:02	33.725	72.383	5.00	3.2
76	9/30/1991	23:48	33.973	72.577	13.50	3.2
77	10/8/1996	0:58	33.734	72.232	14.22	3.2
78	10/26/1998	10:26	34.057	72.784	4.99	3.2
79	11/8/2000	22:45	33.976	72.578	10.82	3.2
80	4/24/2001	4:18	34.132	72.852	9.54	3.2
81	12/8/2002	13:04	34.132	72.852	1.89	3.2
82	11/25/2004	22:31	34.068	72.852	27.58	3.2
83	12/2/2006	19:05	33.959	72.581	8.57	3.2
84	8/18/2007	21:08	34.132	72.950	8.98	3.2
85	11/29/2009	1:53	33.672	72.313	12.29	3.2
86	8/30/1974	16:25	34.000	72.600	0.00	3.1
87	2/25/1976	4:32	34.017	72.600	6.00	3.1
88	11/25/1976	22:23	33.900	72.617	15.00	3.1
89	12/13/1979	9:00	33.958	72.542	26.20	3.1
90	3/31/1981	18:46	34.142	72.900	17.50	3.1
91	6/10/1982	22:12	34.050	72.650	4.30	3.1
92	11/14/1991	7:41	33.887	72.608	14.30	3.1
93	6/1/1996	16:03	33.713	72.350	4.00	3.1
94	7/17/1999	1:56	34.057	72.893	9.00	3.1
95	9/4/2001	21:22	33.734	72.232	5.00	3.1
96	11/18/2002	3:59	33.734	72.232	19.20	3.1
97	5/21/1975	1:42	34.092	72.767	12.50	3.0
98	7/31/1976	7:40	34.043	72.853	13.90	3.0
99	8/26/1979	17:48	34.008	72.708	13.70	3.0
100	8/17/1986	10:48	33.758	72.375	5.00	3.0
101	10/1/1991	10:30	33.985	72.580	10.70	3.0
102	8/1/1993	2:00	34.132	72.923	19.07	3.0
103	1/5/1994	3:56	33.922	72.590	8.04	3.0
104	4/10/1994	13:22	34.072	72.852	10.00	3.0
105	5/7/1995	17:10	34.023	72.740	12.05	3.0
106	2/19/1996	15:20	34.038	72.667	6.05	3.0
107	3/21/1997	3:26	33.734	72.232	5.00	3.0
108	6/15/1997	9:06	34.177	72.871	5.00	3.0
109	6/17/1997	18:25	34.143	72.871	13.76	3.0
110	5/2/2005	4:08	33.734	72.232	5.00	3.0
111	2/21/2009	20:58	33.946	72.532	0.96	3.0

4. Discussion

The aim of this study is to investigate the active faults in the Peshawar Basin, which provide evidence of neo-tectonics. In a previous study by (Hussain and Yeats, 2002) active faults were only recognized in the southern part of the basin. However, this study uses advanced techniques to understand neo-tectonics and active tectonics. Hillshed images derived from Digital Evaluation Model (DEM) were used to identify active faults throughout the Peshawar Basin. The recent evaluation of seismic activity confirms active tectonics. Earthquake data reveals that the Peshawar Basin has experienced more than 1200 earthquakes in the last forty-five years (1973-2018). To make the earthquake data more concise, it was restricted to only marked faults within a radius of 7.5 km, which confirms the marked active faults. It is important to be prepared for earthquakes that occur on certain faults, as they may have longer recurrence periods. Therefore, it is crucial to understand tectonic events over much longer time scales, ranging from several thousand to tens of thousands of years. This will allow for a more in-depth analysis of these processes, leading to improved long-term seismic event prediction. However, there is limited geophysical data available in the Peshawar Basin and the quality of the seismic lines are not very good. Nevertheless, the interpretation of the only three lines that cut the marked faults validates the presence of active faults.

To ensure the authenticity of data interpretation, field evidences are crucial. Therefore, a detailed fieldwork conducted. All of these faults pass through densely populated urban areas, making it the only way to detect fractures, cracks, and subsidence in infrastructure and roads. Fracture data was collected at six points on both sides of each marked active fault.

On the basis of these fracture data analysis, stress direction and faults types were recognized. In the recent deposits, tilting and normal faults were observed. Although these faults were small in scale, they indicate the possibility of larger faults. This study is unique and significant, providing a new direction for active tectonics in the Peshawar Basin.

5. Conclusion

The Peshawar Basin contains six identified faults: Charsadda-Takht Bhai, Mardan, Pir Piai, Pir Sabak, Swabi, and Ghorghasti. To recognize these faults, high-resolution Digital Evaluation Models (DEMs), field observations, seismic line interpretations, and earthquake data have been utilized.

Between August 16, 1973 and December 27, 2018, more than 1200 earthquakes with magnitudes ranging from 3 to 5.7 occurred in the Peshawar Basin. These earthquakes affected various regions along the fault line and took place at different intervals, ranging from one to several years. This suggests that some of these faults may still be periodically active.

Based on the interpretation of fracture data, the Ghorghasti and Pir Sabak faults are thrust faults, whereas the Charsadda-Takhbhai, Mardan, Pir Piai, and Swabi faults are normal faults. Alluvial deposits reveal that normal faults and anticlinal folds are present along these active faults, which supports the wider-scale active deformation.

During fieldwork, subsidence occurred along the Swabi Fault, and tilting of poles and roads along the Ghorghasht Fault was observed. These are signs of active tectonics.

Authors Contribution

Muhammed Irfan Faiz mainly contributed to fieldwork, article write-up, data collection, data analysis, and compilation. Sajjad Ahmed guided at every stage of the work and compilation of the research article. Shuhab D. Khan helped to mark active faults using Hill shade derived from DEM. Fayyaz Ali facilitates fieldwork and research. Gohar Rehman assisted and made valuable contributions to the analysis of Seismic Line interpretation data. Adnan Khalid assisted with formatting, writing, and compiling the manuscript. Taqueemul Haq Ali accompanied and assisted with fieldwork, particularly in the Charsadda region.

Acknowledgments

This article is based on Ph.D. research work of Muhammed Irfan. We would like to thank Nowrad Ali, Adil Khan, and Suleman Khan for their invaluable assistance. Pakistan's Oil and Gas Development Limited supplied six seismic lines. and the Tarbella Seismic Centre, Water and Power Development Authority, provided earthquake data; both departments are acknowledged for this.

References

Cornwell, K., 1998. Quaternary break-out flood sediments in the Peshawar basin of northern Pakistan. Geomorphology, 25(3-4), 225-248.

Davis, J.M., Elston, W.E., and Hawkesworth, C.J., 1993. Basic and intermediate volcanism of the Mogollon-Datil volcanic field: implications for mid-Tertiary tectonic transitions in southwestern New Mexico, USA. Geological Society, London, Special Publications, 76(1), 469-488.

Goscombe, B., Gray, D., and Foster, D.A., 2018. Metamorphic response to collision in the Central Himalayan Orogen. Gondwana Research, 57, 191-265.

Hussain, A., and Yeats, R.S., 2002. Active faulting in the southern Peshawar basin, Pakistan. Geological Bulletin University of Peshawar, 35, 113-124.

Hussain, A., Dipietro, J.A., and Pogue, K.R., 1998. Stratigraphy and structure of the Peshawar basin, Pakistan. Journal of Nepal Geological Society, 18, 25–35.

Kohn, M.J., 2014. Himalayan metamorphism and its tectonic implications. Annual Reviews of Earth and Planetary Science, 42, 381–419. https://doi.org/10.1146/annurev-earth-060313-055005.

Norris, R., Koons, P., and Cooper, A., 1990. The obliquely-convergent plate boundary in the South Island of New Zealand: implications for ancient collision zones. Journal of structural geology, 12(5-6), 715-725.

Searle, M.P., and Schubert, G.B.T.T., 2015. 6.11-Mountain Building, Tectonic Evolution, Rheology, and Crustal Flow in the Himalaya, Karakoram, and Tibet. 469-511.

Searle, M.P., and Treloar, P.J., 2019. Introduction to Himalayan tectonics: a modern synthesis. The Geological Society of London, 483, 1-17.

Slemmons, D.B., and Depolo, C.M., 1986. Evaluation of active faulting and associated hazards. Active Tectonics, 45-62.

Stirling, M., Goded, T., Berryman, K., and Litchfield, N., 2013. Selection of earthquake scaling relationships for seismic-hazard analysis. Bulletin of the Seismological Society of America, 103(6), 2993-3011.

WAPDA, 2018. Earthquake data report.